Near-Infrared Bioimaging

DOI: 10.1002/anie.201004398

Water-Dispersed Near-Infrared-Emitting Quantum Dots of Ultrasmall Sizes for In Vitro and In Vivo Imaging**

Yao He, Yiling Zhong, Yuanyuan Su, Yimei Lu, Ziyun Jiang, Fei Peng, Tingting Xu, Shao Su, Qing Huang, Chunhai Fan,* and Shuit-Tong Lee**

Near-infrared (NIR)-fluorescence imaging is widely recognized as an effective method for high-resolution and high-sensitivity bioimaging because of its minimized biological autofluorescence background and the increased penetration of excitation and emission light through tissues in the NIR wavelength window (700–900 nm).[1] There have been tremendous efforts to develop high-efficiency fluorescent biological probes for NIR-fluorescence imaging.[2] Semiconductor quantum dots (QDs) have attracted much recent attention as a new generation of fluorescent probes because of their unique optical properties such as strong luminescence, high photostability, and size-tunable emission wavelength.[3] While QDs emitting in the range of 450–650 nm have been well developed,[3,4] NIR-emitting QDs have been much less explored because of their relatively complicated synthesis and post-treatment manipulations. Furthermore, NIR-emitting QDs are usually prepared in organic phase, and additional surface modification is employed to render them water-dispersible for biological applications.[5] The relatively complicated surface modification often results in an increase in size of the QDs.[6] Only recently, water-dispersed NIR-emitting CdTe/CdS QDs with tetrahedral structure were directly prepared in aqueous phase through the epitaxial-shell-growth method.[5c] Despite these advances, much work is still needed to obtain NIR-emitting QDs that can be facilely synthesized in aqueous phase for high-sensitivity and specific bioimaging.

Herein, we report the first example of ultrasmall-sized NIR-emitting CdTe QDs with excellent aqueous dispersibility, robust storage, chemical, and photostability, and strong photoluminescence (photoluminescent quantum yield (PLQY): 15–20%). Significantly, the NIR QDs are directly synthesized in aqueous phase through a facile one-step microwave-assisted method (see the Supporting Information for experimental details and mechanisms) by utilizing several attractive properties of microwave irradiation such as prompt startup, easy heat control (on and off), prompt and homogeneous heating, and so forth.[7] More importantly, highly spectrally and spatially resolved bioimaging was possible, and efficient tumor passive targeting in live mice was shown by using the prepared QDs.

QDs with different emission wavelengths in the NIR range ($\lambda_{max} = 700$–800 nm) can be readily prepared through fine adjustment of the experimental conditions (e.g., reaction time and temperature). Figure 1a,b displays the normalized ultraviolet photoluminescence (UV-PL) spectra for a series of as-prepared QDs with controllable maximum emission wavelength ranging from 700 to 800 nm in aqueous solution. Such QD solutions are transparent under ambient light conditions, suggesting the as-prepared QDs are well-dispersed in aqueous phase without further treatment (Figure 1c). The excellent aqueous dispersibility of the QDs arises from the surface-covering mercaptopropionic acid (MPA) that acts as a stabilizer because of the presence of negatively charged carboxylic groups.[8] Under UV irradiation the fluorescence of the as-prepared QDs became darker and the emission wavelength gradually shifted out of the visible region (Figure 1d).

The transmission electron microscopy (TEM) and high-resolution TEM (HRTEM) images reveal that the NIR-emitting QDs are spherical particles with good monodispersibility (Figure 2a,b). The existence of a well-resolved crystal lattice in the HRTEM image further confirms the highly crystalline structures of the QDs (Figure 2b inset). Furthermore, the size distribution histogram (Figure 2c), which was determined by measuring more than 250 particles, shows that the average size and standard deviation of the as-prepared NIR-emitting QDs is (3.74 ± 0.67) nm. Comparatively, the

[*] Prof. Y. He, Y. L. Zhong, Dr. Y. Y. Su, Y. M. Lu, Z. Y. Jiang, F. Peng, T. T. Xu, Dr. S. Su
Institute of Functional Nano & Soft Materials (FUNSOM)
and Jiangsu Key Laboratory for Carbon-Based Functional Materials & Devices, Soochow University
Suzhou, Jiangsu 215123 (China)
Fax: (+86) 512-6588-2846
E-mail: yaohe@suda.edu.cn

Prof. Y. He, Dr. Y. Y. Su, T. T. Xu, Prof. S. T. Lee
Center of Super-Diamond and Advanced Films (COSDAF)
and Department of Physics and Materials Science
City University of Hong Kong
Hong Kong (P. R. China)
Fax: (+852) 2-784-4696
E-mail: apannale@cityu.edu.hk

Dr. S. Su, Prof. Q. Huang, Prof. C. H. Fan
Laboratory of Physical Biology
Shanghai Institute of Applied Physics
Chinese Academy of Sciences, Shanghai 201800 (China)
E-mail: fchh@sinap.edu.cn

[**] We appreciate financial support from the Research Grants Council of HKSAR (grant number CityU5/CRF/08), the RGC-NSFC Joint Research Scheme (grant number N_CityU108/08), the Ministry of Health (grant number 2009ZX10004-301), the NSFC (grant numbers 30900338, 20725516, and 51072126), and a project funded by the priority academic program development of the Jiangsu Higher Education Institutions (PAPD). We thank Prof. L. S. Liao and Prof. L. H. Wang for fruitful discussions, and Dr. Y. B. Tang for technical help.

Supporting information (including experimental details) for this article is available on the WWW under http://dx.doi.org/10.1002/anie.201004398.

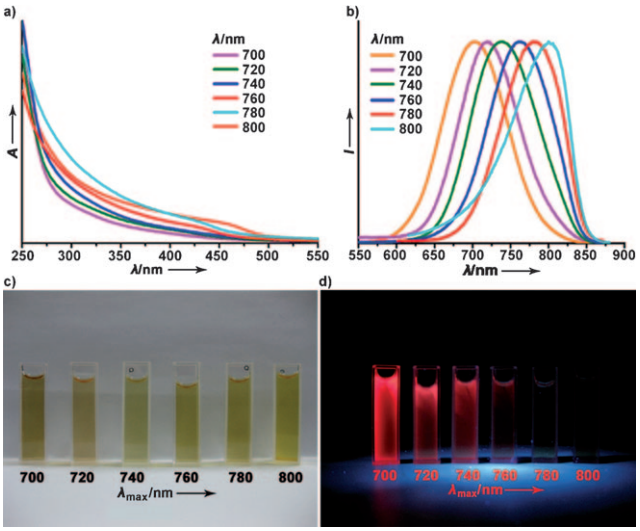

Figure 1. a,b) Series of UV-PL spectra of the NIR-emitting QDs with controllable maximum emission wavelengths ranging from 700–800 nm ($\lambda_{excitation} = 450$ nm). Photographs of the aqueous solution of QDs under c) ambient light conditions and d) UV irradiation ($\lambda_{excitation} = 365$ nm). The samples were directly extracted from the original solution right after reaction without further treatment.

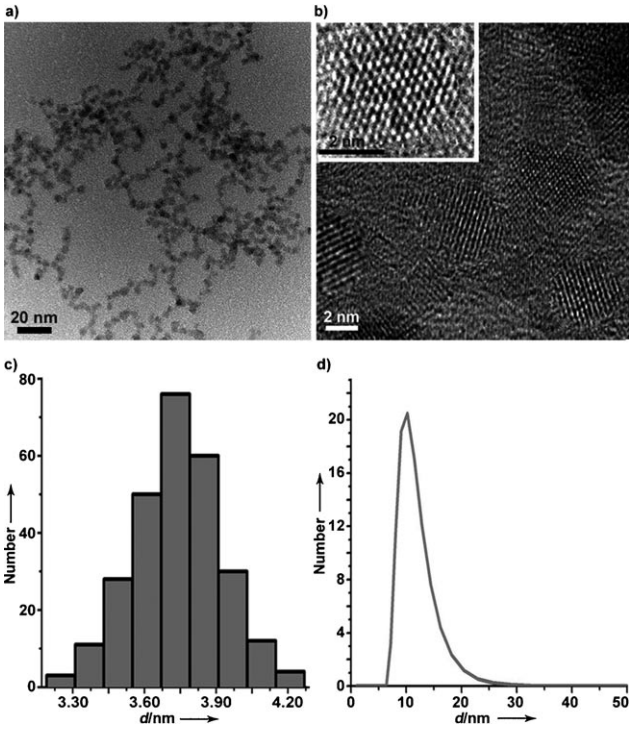

Figure 2. a) TEM and b) HRTEM images (scale bar in the inset: 2 nm), as well as c) the size distribution, and d) dynamic light-scattering histogram of the prepared NIR-emitting QDs ($\lambda_{emission} = 740$ nm).

corresponding hydrodynamic diameter of the QDs in water is around 10 nm, as measured by dynamic light scattering (DLS; Figure 2d). The difference in diameter measured by TEM and DLS is attributed to different surface species of the as-prepared QDs in aqueous phase.[8a,9] Importantly, the ultra-small size offers great advantages for bioimaging compared to conventional NIR QDs with larger sizes (DLS: 15–30 nm; see the Supporting Information for a detailed discussion).[5]

As shown in Figure 3a, powder X-ray diffraction (XRD) characterization indicates that the prepared NIR-emitting

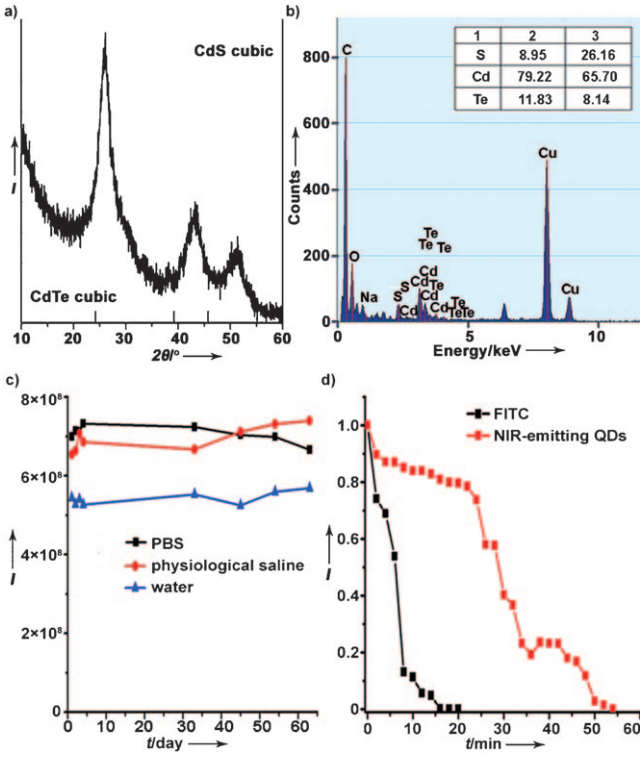

Figure 3. a) XRD and b) EDS pattern of the NIR-emitting QDs (in the table: 1 = element, 2 = weight fraction, and 3 = atomic fraction). c) Temporal evolution of the PL intensity of the QDs over two months in water, PBS, and physiological saline, respectively. d) Photostability of FITC and the NIR-emitting QDs. The samples were continuously irradiated by a xenon lamp (365 nm, 450 W).

QDs belong to the cubic (zinc) structure, which is also the dominant crystal phase of bulk CdTe. The positions of the XRD reflections are intermediate between the values of cubic CdTe and CdS phase (see the Supporting Information for a detailed discussion). Energy-dispersive spectrometry (EDS) measurements clearly indicate the presence of cadmium, tellurium, and sulfur with relative weight fractions of 79.22%, 11.83%, and 8.95%, respectively, and prove further the formation of mixed CdTe(S) QDs (Figure 3b).

The stability of fluorescent probes is critically important for biological applications.[3,10] Significantly, our NIR-emitting QDs display superior storage, chemical, and photostability. The QDs retained almost the original fluorescent intensity after storage in water for two months. The as-prepared QDs were similarly stable when dispersed in either phosphate-buffered saline (PBS, 0.15 M) or physiological saline with minimal fluorescence decrease (ca. 10%; Figure 3c). Specifically, the PL intensity of the QDs in PBS or aqueous solution slightly increased after storage for 30 days, and then gradually decreased to the original intensity after storage for 60 days. The PL intensity of the QDs in physiological saline kept the

slight increase during the 60 days of storage, and then decreased to the original intensity after storage for 80 days (data not shown). The PL intensity of the QDs is enhanced by the formation of CdS shells (see the Supporting Information for a detailed discussion).

We further evaluated the photostability of the as-prepared QDs. Figure 3d shows that the fluorescence of fluorescein isothiocyanate (FITC, an organic dye) rapidly dropped to only 20% of the original fluorescence intensity in merely 8 min, and became negligible after 15 min. In sharp contrast, the fluorescence of the QDs was remarkably stable and decreased only slightly under UV irradiation retaining > 80% of the original intensity even after irradiation for 25 min. This comparison indicates a superior photostability of the NIR-emitting QDs similar to conventional QDs which makes their use for long-term and real-time bioimaging applications possible.[3]

To demonstrate their utility as NIR-emitting biological probes, we further employed our NIR QDs for both in vitro and in vivo imaging. Importantly, the as-prepared QDs can be conveniently functionalized with antibodies since they contain a number of surface carboxylic groups.[8] Our QDs were shown to be chemically stable when conjugated with antibodies. The resultant NIR-QDs/protein bioconjugates were further applied for targeted immunological cell imaging. Significantly, the NIR-emitting QDs ($\lambda_{max} = 780$ nm) conjugated with a goat anti-mouse antibody were first employed for immunofluorescent targeting of cellular microtubules. Figure 4a–d shows that Hela cells are distinctively dually labeled with the QD bioconjugates and a blue-colored nuclei-specific Hoechst (a commercially available organic dye). The photoluminescence of the bioconjugate-labeled Hela cells is very bright and clearly spectrally resolved.

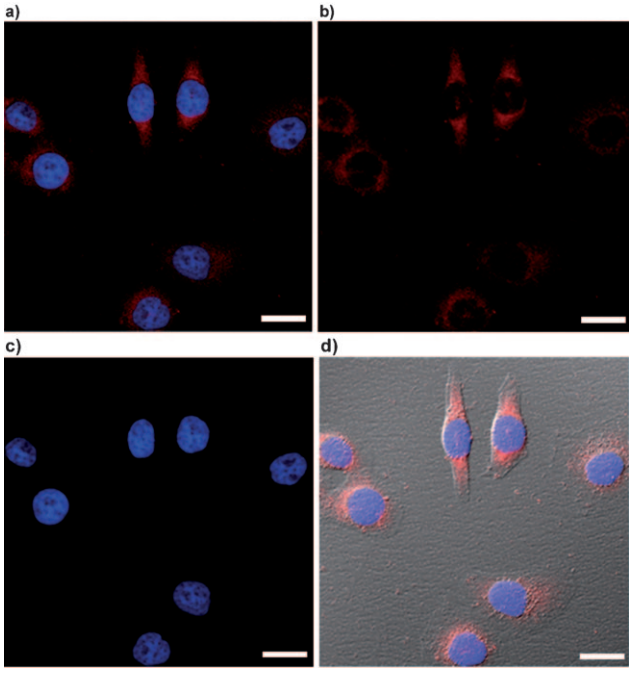

Figure 4. a)–d) Dual-color immunofluorescent cellular imaging photos (scale bar: 20 μm). The Hela cells are distinctively labeled by the QDs/protein bioconjugates (red) and Hoechst (blue): a) 458 nm excitation, detection window: 740–950 nm, b) 405 nm excitation, detection window: 420–500 nm, c) superposition of the fluorescence images with 405 and 704 nm excitation, and d) superposition of all fluorescence and transillumination images.

In addition to utilization of the NIR QDs for cellular labeling, we employed the NIR-emitting QDs for in vivo imaging. The NIR QDs were subcutaneously injected into the back of a mouse, and then examined by in vivo imaging. Significantly, the fluorescent signals of the QDs were distinctively bright, clearly spectrally and highly spatially resolved, despite the presence of a strong autofluorescence background in the mouse (Figure 3e,f). This study clearly demonstrates the advantages of NIR QDs for in vivo imaging for which the QD fluorescence and biological autofluorescence of the mouse are spectrally separated, and that the NIR emission is less absorbed by tissue than visible luminescence.[1,5] To further investigate the chemical stability of the QDs in vivo, the NIR QDs were intravenously injected into the tail vein of the mouse. Most QDs were found to be accumulated in the liver 0.5 h after the injection. The liver was then carefully collected and its fluorescence was examined. Importantly, with comparison to the feeble autofluorescence of a control group, the liver with QD accumulation displayed bright fluorescent signals (Figure 5c and d), indicating that

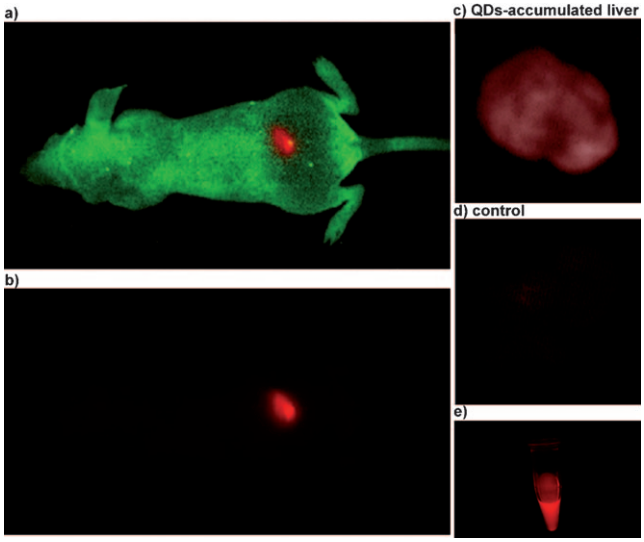

Figure 5. High spectral and spatial sensitivity of QD imaging in a live mouse in the a) presence and b) absence of biological autofluorescence. c) In vivo fluorescence image of the liver after QD accumulation. d) A control image of the liver before injection of QDs is given for comparison. e) Strong fluorescence of the QDs in the imaging equipment.

the NIR-emitting QDs are highly stable in the complex biological environment. We administered the QDs to tumor-bearing mice through intravenous injection. The injected QDs were monitored by measuring time-lapse in vivo NIR images. We observed a color change in the tumor region from black to olive during 6 h of blood circulation where the olive color denotes much stronger absorption than the black color. The results indicate high accumulation of the QDs in the tumor region through a passive targeting process caused by an

enhanced permeability and retention (EPR) effect.[11] To our knowledge, this is the first example of in vivo tumor targeting by using water-dispersed QDs directly prepared in aqueous phase (Figure 6).

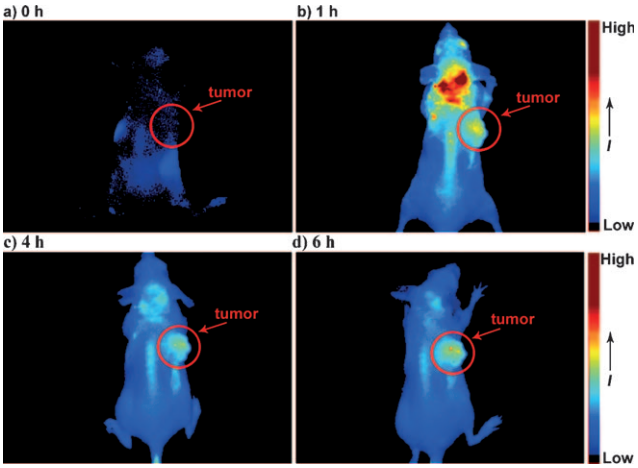

Figure 6. In vivo tumor targeting of the NIR QDs. Spectrally unmixed in vivo fluorescence images of a KB-tumor-bearing nude mice at a) 0, b) 1 h, c) 4 h, and d) 6 h after injection of the prepared QDs. The autofluorescence of the mouse was removed by spectral unmixing of the above images. A high uptake of QDs by the tumor was observed.

In summary, water-dispersed NIR-emitting ultrasmall-sized CdTe QDs were directly prepared in aqueous phase through a facile one-step microwave synthesis. The QDs display excellent aqueous dispersibility, high storage, chemical, and photostability, and a finely tuneable emission in the NIR range (700–800 nm). The QDs can readily be functionalized with antibodies to produce biologically functional QD–protein conjugates. Of particular significance is that systematic in vitro and in vivo imaging data demonstrate that the prepared NIR QDs are especially suitable for highly spectrally and spatially resolved imaging in cells and animals. Moreover, in vivo tumor targeting using the water-dispersed NIR QDs was shown for the first time. In comparison to conventional NIR QDs of larger sizes, our ultrasmall QDs offer great opportunities for highly specific, efficient, and sensitive bioimaging. These unprecedented advantages may render the NIR-emitting QDs promising tools for in vitro and in vivo NIR-fluorescence imaging applications.

Received: July 19, 2010
Revised: April 8, 2011
Published online: May 9, 2011

Keywords: imaging agents · microwave chemistry · quantum dots · tumors

[1] a) R. Weissleder, *Nat. Biotechnol.* **2001**, *19*, 316–317; b) R. Weissleder, V. Ntziachristos, *Nat. Med.* **2003**, *9*, 123–128; c) S. Lee, E. J. Cha, K. Park, S. Y. Lee, J. K. Hong, I. Sun, S. Y. Kim, K. Choi, I. C. Kwon, K. Kim, C. H. Ahn, *Angew. Chem.* **2008**, *120*, 2846–2849; *Angew. Chem. Int. Ed.* **2008**, *47*, 2804–2807.
[2] a) A. Zaheer, R. E. Lenkinski, A. Mahmood, A. G. Jones, L. C. Cantley, J. V. Frangioni, *Nat. Biotechnol.* **2001**, *19*, 1148; b) W. Jiang, E. Papa, H. Fischer, S. Mardyani, W. C. W. Chan, *Trends Biotechnol.* **2004**, *22*, 607–609.
[3] X. Michalet, F. F. Pinaud, L. A. Bentolila, J. M. Tsay, S. Doose, J. J. Li, G. Sundaresan, A. M. Wu, S. S. Gambhir, S. Weiss, *Science* **2005**, *307*, 538–544.
[4] a) L. Qu, X. G. Peng, *J. Am. Chem. Soc.* **2002**, *124*, 2049–2055; b) L. Manna, J. Milliron, A. Meisel, E. C. Scher, A. P. Alivisatos, *Nat. Mater.* **2003**, *2*, 382–385.
[5] a) S. Kim, Y. T. Lim, E. G. Soltesz, A. M. De Grand, J. Lee, A. Nakayama, J. A. Parker, T. Mihaljevic, R. G. Laurence, D. M. Dor, L. H. Cohn, M. G. Bawendi, J. V. Frangioni, *Nat. Biotechnol.* **2003**, *22*, 93–97; b) J. P. Zimmer, S. W. Kim, S. Ohnishi, E. Tanaka, J. V. Frangioni, M. G. Bawendi, *J. Am. Chem. Soc.* **2006**, *128*, 2526–2527; c) Z. Deng, O. Schulz, S. Lin, B. Ding, X. Liu, X. Wei, R. Ros, H. Yan, Y. Liu, *J. Am. Chem. Soc.* **2010**, *132*, 5592–5593.
[6] a) S. T. Selvan, T. T. Tan, J. Y. Ying, *Adv. Mater.* **2005**, *17*, 1620–1625; b) H. M. Wu, H. Z. Zhu, J. Q. Zhuang, S. Yang, C. Liu, Y. C. Cao, *Angew. Chem.* **2008**, *120*, 3790–3794; *Angew. Chem. Int. Ed.* **2008**, *47*, 3730–3734.
[7] a) D. Michael, P. Mingo, D. R. Baghurst, *Chem. Soc. Rev.* **1991**, *20*, 1–47; b) S. A. Galema, *Chem. Soc. Rev.* **1997**, *26*, 233–238.
[8] a) Y. He, Kang. Z. H. Q. S. Li, C. H. A. Tsang, C. H. Fan, S. T. Lee, *Angew. Chem.* **2009**, *121*, 134–138; *Angew. Chem. Int. Ed.* **2009**, *48*, 128–132; b) Y. He, Y. Y. Su, X. B. Yang, Z. H. Kang, T. T. Xu, R. Q. Zhang, C. H. Fan, S. T. Lee, *J. Am. Chem. Soc.* **2009**, *131*, 4434–4438; c) Y. He, C. H. Fan, S. T. Lee, *Nano Today* **2010**, *5*, 282–295; d) Y. He, Y. L. Zhong, F. Peng, X. P. Wei, Y. Y. Su, S. Su, W. Gu, L. S. Liao, S. T. Lee, *Angew. Chem.* **2011**, *123*, 3136–3139; *Angew. Chem. Int. Ed.* **2011**, *50*, 3080–3083.
[9] S. S. Banerjee, D. H. Chen, *Chem. Mater.* **2007**, *19*, 6345–6349.
[10] a) C. M. Niemeyer, *Angew. Chem.* **2001**, *113*, 4254–4287; *Angew. Chem. Int. Ed.* **2001**, *40*, 4128–4158; b) M. Green, *Angew. Chem.* **2004**, *116*, 4221–4223; *Angew. Chem. Int. Ed.* **2004**, *43*, 4129–4131; c) R. Gill, M. Zayats, I. Willner, *Angew. Chem.* **2008**, *120*, 7714–7736; *Angew. Chem. Int. Ed.* **2008**, *47*, 7602–7625.
[11] a) S. M. Lee, H. Park, K. H. Yoo, *Adv. Mater.* **2010**, *22*, 4049–4053; b) K. Yang, S. Zhang, G. X. Zhang, X. M. Sun, S. T. Lee, Z. Liu, *Nano Lett.* **2010**, *10*, 3318–3323.

